Scientia Iranica B (2023) 30(1), 30–38

SCIENTIA IRANICA

Sharif University of Technology
Scientia Iranica
Transactions B: Mechanical Engineering
http://scientiairanica.sharif.edu

Investigation of the effect of arteriole clogging of the heart on the characteristics of intravenous blood flow

W. Long[a], R. Margiana[b,*], Z. Haleem Al-qaim[c], O.K.A. Alkadir[d], R.M. Romero Parra[e], and A. Ghanbarzadeh Kojan[f]

a. *College of Chemistry, Guangdong University of Petrochemical Technology, Maoming 525000, PR China.*
b. *Faculty of Medicine, Universitas Indonesia, Jakarta, Indonesia; and Soetomo General Academic Hospital, Surabaya, Indonesia.*
c. *Department of Anesthesia Techniques, Al-Mustaqbal University College, Hillah, Iraq.*
d. *Al-Nisour University College, Baghdad, Iraq.*
e. *Department General Studies, Universidad Continental, Lima, Perú.*
f. *Faculty of Medicine, Islamic Azad University, Ardabil Branch, Ardabil, Iran.*

Received 17 January 2022; received in revised form 17 May 2022; accepted 1 August 2022

KEYWORDS
Clogging of arteries;
Blockage;
CFD analysis;
Blood flow.

Abstract. In this paper, the behavior of blood flow through several consecutive and relatively close clogs inside the vessel is investigated by modeling blood vessels. The used clogs are dual-channel and single-channel currents, which are naturally very close. Consecutive clogs with equal intervals and different clogs of 30%, 50%, and 70% are considered. The inflow to the clogged area is in the form of a real pulse, the same as the pulse of blood flow in a vein. For this purpose, the *Navier-Stokes* equations are solved numerically in an unstable state, while the continuity equation in the capillary coordinate system is solved by the numerical method. The distribution of flow velocity and distribution of shear and vertical stresses in the vessel wall in three states of the flow cycle are related to the acute conditions of the cyclic blood flow. The results show that the rate of increase in shear stresses and the rate of decrease in vertical stresses become much more severe upon increasing the rate of clamping. These changes are more severe at distances of 17 mm for two channels and 25 mm for single channels, which have a maximum blood flow rate.

1. Introduction

In order to prevent and treat heart disease, simulation and modeling of the heart and coronary arteries are of significance in medical engineering. Software and computational techniques such as Finite Element Method (FEM) are employed to evaluate the blood flow and heart performance. Therefore, it is important to apply FEM to clogged arteries [1–5]. Arteries are thick-walled and carry oxygen-rich blood to vital tissues and organs. The arterial branches get smaller and smaller to become capillaries, which form only one cell. The capillary bed is where the blood exchanges oxygen and nutrients with the body's tissues and collects waste products. The return of blood from the capillaries to the heart is done through the veins [6]. Veins have a thinner vascular wall than the arteries and the flow of blood in them is low. Arteries and veins often run in parallel and opposite directions and are not directly related to each other. In fact, they are separated by capillary networks in body tissues, and there are special control systems that prevent the formation of untimely arterial connections. Venous artery malformation is a

*. *Corresponding author. Tel.: 62-21-727-0020*
E-mail address: riariamargiana@gmail.com (R. Margiana)

doi: 10.24200/sci.2022.59767.6412

set of abnormally intertwined vessels fed by arteries and drained by veins without capillaries interfering. As a result, a significant low-resistance flow occurs that directs blood from the arterial system directly to the venous system [7,8]. The veins are unable to control the high-pressure blood entering the arteries and become larger and larger as they accept more blood. As a result, the veins weaken over time and the risk of rupture and bleeding increases.

Different studies [9–12] evaluated the blood flow in the vein to predict the pressure and health of human. Assuming blood flow as a non-Newtonian fluid, they proposed a mathematical model for blood flow along the artery. They considered the artery to be inelastic and the geometry to be clogged independent of time. In this study, blood flow is assumed to be pulsed, incompressible, and symmetrically centered, and the governing equations of flow are solved by the perturbation method. In [13], blood flow was considered to be non-Newtonian, pulsed, and non-continuous fluid. The arteries assumed in this study were assumed elastic, and the governing equations of blood flow were solved using the finite difference method. Blood as a Newtonian fluid does not have the ability to accurately describe the properties of blood flow. The assumption that blood flow is Newtonian for flow with high shear strain is acceptable, which is true for flow along vessels with an inner diameter greater than one millimeter. In [14], considering a catheter in the cone vein, micropolar fluid was used for the vein with mild obstruction. Authors in [15] used the hypothesis of mild occlusion in their study of the mathematical modeling of pulsed blood flow in an asymmetric occlusion vessel with a catheter, the effect of a conical angle, and the slip velocity.

Several numerical simulations [16–20] were performed with the aim of investigating blood flow and shear stresses in the adjacent wall of mono-stenosis at different degrees involved in the main, lateral, and terminal branches, as well as observing the pulsating blood flow inside. The results obtained in [20] illustrated that blood flow in the arterial areas in the range of rheological effects, especially in the case of 90% obstruction, had non-Newtonian properties. Numerical simulations of blood flow at different viscosities were performed in [21]. This explains the completed simulations with 10 to 80% occlusions at different Reynolds numbers of 50, 100, 500, 1000, and 4000. The results demonstrate how these parameters might change in the critical condition stage due to clogged arteries. In [22], an analytical solution for the deformation of human arteries was presented. The blood vessel was modeled as a homogeneous isotropic cylinder in which its incompressible stress-strain behavior was investigated. Their results include changes in diameter and thickness with stress distribution for both monolayer and bilayer models, indicating a major difference between monolayer and bilayer models in stress distribution. In [23], the stress distribution in the abdominal aortic aneurismal wall was investigated using finite element modeling. The results of this study indicate that in addition to the size of the aneurysm, mechanical properties and blood flow may also significantly affect the stress distribution in the aneurismal wall. In [24], hemodynamic analysis, complete coronary artery bypass grafting with elastic walls, and different percentages of stenosis were investigated numerically. The effects of wall tension, current pulsability, and stenosis percentage on flow configuration, Wall Shear Stress (WSS), and rotational currents were presented. Their results indicate that WSS produces lower values in the toe, heel, and bed of the branching host vessel in the elastic state, which is closer to reality. It is also concluded that upon increasing the percentage of stenosis, the probability of rotational flow increases.

Modeling blood flow in the human vascular system helps physicians to understand vascular disease better and how it develops and to make important decisions before surgery [25–27]. One of the methods of modeling blood flow in the vascular system of the human body and related diseases is mechanical modeling and using blood flow simulation. One of the new researches in the field of simulation of blood flow in arteries and related diseases is the use of blood flow simulation technology and bypass method. In this study, numerical simulation of blood flow in arterial disease of clogged arteries for a real geometry using computational dynamics technology and flow field variables will be investigated.

2. CFD Modelling

2.1. Fluid flow equations

CFD was used for the numerical solution in the present research. The averaged three-dimensional, steady-state, and compressible Navier-Stokes equations and the mass conservation equations, represented by Eqs. (1) and (2), were solved using the finite volume method [28].

$$\frac{\partial \rho U_i}{\partial t} + \frac{\partial}{\partial x_j}(\rho U_i U_j) = \frac{\partial p}{\partial x_i} + \frac{\partial}{\partial x_j}\left[\mu_{eff}\left(\frac{\partial U_i}{\partial x_j} + \frac{\partial U_j}{\partial x_i}\right)\right] + S_M, \quad (1)$$

$$\frac{\partial \rho}{\partial t} + \frac{\partial(\rho U_i)}{\partial x_i} = 0. \quad (2)$$

In these equations, U_i denotes the average component of the flow velocity, U_i fluctuating component of flow velocity, and $\rho(U_i U_j)$ Re stress tensors, S_M the sum

of the body forces, and μ_{eff} is the effective viscosity. The above equation system was completed for the numerical solution by modeling the stresses via the shear stress transport turbulence model.

2.2. Modeling a clogged vessel

In the present study, a red blood vessel with a diameter of 6 mm and a length of 11 cm was selected to evaluate the movement of blood and clots in partially clogged arteries. Table 1 presents the simulation results.

In order to consider the effect of clogging, two types of clogging with cylindrical and cubic platelets are examined. Clogged artery is assumed that there is a symmetrical clogging at a distance of 4 cm from the entrance of this vessel. The geometry of the desired vessel is produced by CAD model and Figure 1 shows an example of this created geometry.

Blood is a fluid tissue consisting of 55% plasma and 45% blood cells. These components have different densities, the density of blood cells is 1025 kg/m^3, and the density of blood cells is 1125 kg/m^3. In the present study, the density value for the whole blood was considered 1060 kg/m^3. The boundary walls are not movable and no slippage is observed on the walls; therefore, the velocity in the wall is assumed to be negligible. On the inner side, the flow is fully developed and the pressure on the outside is assumed to be zero. For analysis, the type of solvent is selected based on pressure. In this study, the flow equations are discretized by the volume control method and solved by the SIMPLE algorithm. In the discretization of the equations, the central difference approximation and hybrid approximation are used for infiltration and displacement sentences, respectively, while the latter is used here. In the pressure sentence approximation, the central difference approximation is used in the momentum equation. The convergence criterion is considered for the components of velocity 10–9 and pressure 7–10, and the sub-release coefficients for the components of velocity and pressure are 0.6 and 0.3, respectively.

Table 1. Specification of a clogged vessel with a stent.

Vein length	30 mm
Vein height	5 mm
Blood velocity	0.2 m/s
Blood density	1060 kg/m^3
Blood viscosity	3.5×10^{-3} Pa.s
Type of flow	Laminar
Including gravity	Yes

2.3. Boundary condition

This study considers symmetrical-axial, pulsed, non-continuous, two-dimensional, and fully dilated blood flows along the artery. The type of clamp is considered asymmetrical with respect to the axial direction, but symmetrical with respect to the radial direction. The artery wall is considered elastic and the blood flow is modeled as a bilayer fluid. Dimensional geometry depending on the clogging time in the lateral layer is expressed as Eq. (3) [29–31]:

$$R(z,t) = \begin{cases} a_1(t) & OW \\ 1 - A[l_0^{n-1}(z-d)(z-d)^n]a_1(t), & \\ d \le z \le d + l_0 & \end{cases} \quad (3)$$

where R and A are the radii of the vessel blocked in lateral and central parts, respectively, In addition, L, l_0, and d are the desired vessel length, the length of the blockage, and the length of the upstream area, respectively.

In this two-equation turbulence model, the turbulence kinetic energy and frequency equations are given in Eqs. (4) and (5) [32,33]:

$$\frac{\partial(\rho k)}{\partial t} + \frac{\partial(\rho U_i k)}{\partial x_j} = \bar{P}_k - \beta^* \rho k\omega + \frac{\partial}{\partial x_i}\left[(\mu + \sigma k \mu t)\frac{\partial k}{\partial x_i}\right], \quad (4)$$

$$\frac{\partial(\rho\omega)}{\partial t} + \frac{\partial(\rho U_i \omega)}{\partial x_i} = \left[\frac{5}{9}F_1 + \frac{44}{(1-F_1)}\right]\frac{1}{v_t}\bar{P}_k - \beta\rho\omega^2$$

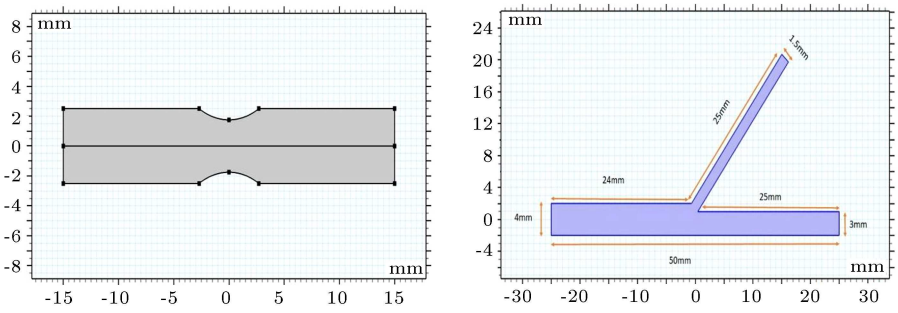

Figure 1. The geometry of a cube-shaped platelet created.

$$+\frac{\partial}{\partial x_i}\left[(\mu++\sigma\omega\mu_t)\frac{\partial\omega}{\partial x_i}\right]$$

$$+2(1-F1)\frac{\rho\sigma_{\omega^2}}{\omega}\frac{\partial k}{\partial x_i}\frac{\partial\omega}{\partial x_i}. \quad (5)$$

The Re stresses are computed in this model using the Boussinesq approximation [34] according to Eq. (6):

$$U_iU_j=-v_t\left(\frac{\partial U_i}{\partial x_j}+\frac{\partial U_j}{\partial x_i}\right)+\frac{2}{3}k\delta_{ij}. \quad (6)$$

The turbulence kinematic viscosity in this relationship is determined using Eq. (7):

$$v_t=\frac{a_1k}{\max(a_1\omega.\sqrt{2S_{ij}S_{ij}}.F_2)}. \quad (7)$$

The blending functions F_1 and F_2 were obtained through Eqs. (8), (9), and (10):

$$F_1=\tanh\left\{\left\{\min\left[\max\left(\frac{\sqrt{k}}{\frac{9}{\varpi y}}.\frac{500v}{\omega^2y}\right).\frac{4\rho\sigma_{w^2}k}{CD_{k\omega}Y_2}\right]\right\}^4\right\}, \quad (8)$$

$$F_2=\tanh\left[\left[\max\left(\frac{2\sqrt{k}}{\frac{9}{\varpi y}}.\frac{500v}{\omega^2y}\right)\right]^2\right], \quad (9)$$

$$CD_{k\omega}=\max\left(.\frac{2\rho\sigma_{w^2}}{\omega}\frac{\partial k}{\partial xi}.\frac{\partial\omega}{\partial xi}.10^{-10}\right). \quad (10)$$

In CFD, the fluid domain of the impeller was defined as a rotating domain at a speed of 85907 RPM, and the other domains (inlet and outlet extensions and the diffuser levels [35]) were defined as stationary ones. All the rigid walls were modeled using the smooth wall and no-slip boundary conditions, and the surface roughness effects were ignored. For further simplification and to ensure a reduction in the computational costs, the rotating domain of the impeller was solved alternatively. The general connection interface was used at the joints between the stationary components, and the frozen rotor interface was used at the joints between the rotating and stationary components. It is worth noting that the alternating fan interface was set to a rotational periodicity interface. Moreover, the mass flow rate and pressure boundary conditions were considered at the inlet and outlet of the fan. The working fluid was assumed to be air at 25°C with a dynamic viscosity of 0.00001825 Pa.s and under ideal gas conditions. The advection and turbulence terms were discretized using the high-resolution scheme, and the convergence criterion of the mass and momentum conservation equations was set to $10e^{-5}$ in CFD.

3. Results

The outcomes of CFD analyses performed on vessels with cubic and cylindrical platelets in which the stent is placed are reviewed. In the previous section, how to perform modeling in CFD with border conditions and entry speed and blood characteristics was explained, while in this section, the effect of clogging and its type on the characteristics of intravenous blood flow is investigated.

3.1. The convergence of results and the independence of the network

In the process of examining the solution independence from the network, the goal is to find the largest network that can be used to simulate the desired function with good accuracy. Therefore, the accuracy of the solution depends entirely on the structure and size of the network and the mesh, and as the number of network cells increases, the computational volume and time required for the simulation increase. The properties of the meshed model are presented in Table 2 and Figure 2.

The first step in examining the independence of the solution from the network is to generate a large-sized network and perform simulations using it. Under these conditions, after the convergence of the solution, the desired result (such as shear strain) is recorded. Here, the desired result is a parameter that is to be compared between different networks in examining the process of solution independence from the network. Figure 3 shows the process of checking the solution independence of the lattice for a cube-plate plate

Table 2. Properties of the meshed model.

Mesh type	Number of meshes	Average mesh quality	Pressure (Pa)	Difference percentage (%)
Extremely coarse	2431	0.7999	28.6	70.2
Coarser	3484	0.839	23.5	67.5
Coarse	5548	0.8641	19.1	13.6
Normal	10224	0.884	17.2	2.3
Fine	25066	0.9297	16.8	0

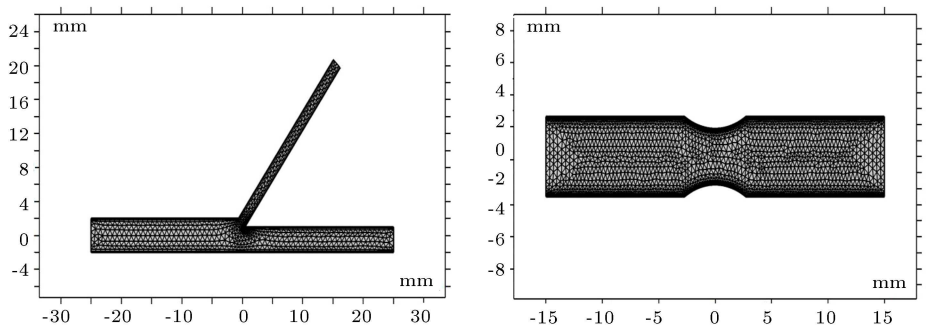

Figure 2. Meshing size of the proposed models.

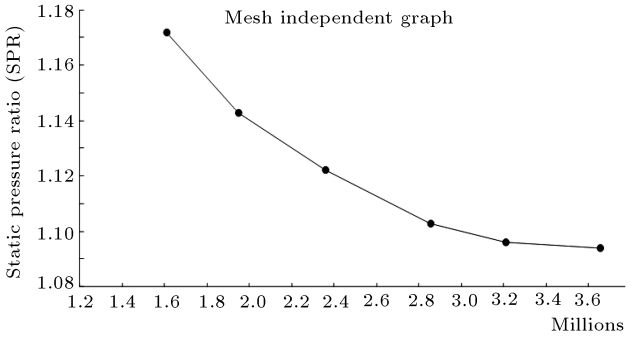

Figure 3. Process of checking the solution independence of the lattice for a cube-shaped plate without a stent.

without a stent. As can be seen, upon increasing the number of elements from about 0.7 million elements, the shear strain results converge to 200 and accordingly, in the analysis of the present study, this number of elements is used.

3.2. Effect of clogged percentile

In this section, the present problem simulates blood flow in a clogged artery. The operating fluid used in the simulation process is blood, which has a density of 1060 kg/m^3 and a viscosity of 0.35 kg/m^3. The flow rate of blood entering the artery from both inlet branches is 0.0024 kg/s, and the vessel wall is assumed to be stationary. A function related to the curvature line is used to define and plot the clogged area inside the vessel. This function represents a set of points x and y forming a curvature line obtained using this relation ($y = 0.0002475\cos((\pi\ x)/0.001)$. It is 30–50%, which means that the ratio of the diameter of the vessel in the clogged area to the total diameter of the vessel is 0.7-0.5-0.3, as presented in Figures 4 and 5.

To compare the effects of clogging on the velocity and pressure disturbance, their variation over the vessel length is presented in Figure 6. As shown, the pressure drops by 40% in the clogged arteries of 0.7, whilst its variation in the clogged condition of 0.3 is close to 5%. It can be found that increase in blockage rate will affect the vein blood flow, which can cause a serious problem.

The hemodynamics of the artery was explained in terms of maximum pressure and velocity through the vein length. Consecutively, there was the addition of different percentages of asymmetric blockages set at parameters of 30%, 50%, and 70% for a straight vein. The pressure drop and velocity variation in the blockage part are evident, which can be a serious problem in blood flow. One method for solving the clogged problem is bypass which is simulated in Figures 7 and 8.

The hemodynamics of the artery has been explained in term of maximum pressure and velocity through the vein length. Consecutively, there was addition of different percentage of asymmetric blockages set at parameters of 30%, 50%, and 70% for straight vein. The pressure drop and velocity variation in the blockage part is evident, which can be serious problem in blood flow. For solving this clogged one method is bypass which simulated in Figures 7 and 8.

The two-vein simulation was considered. For this simulation, the model for the heart vessel was considered first and the effect of the two channels was compared. As shown in Figure 7, the maximum velocity occurs at 28 mm (0.31 m/s) of the length as the starting point of the channel, whereas the pressure drops up to 14 pa.

4. Conclusion

In this simulation, blood flow as a non-neon fluid within an artery was modeled and simulated by the computational dynamics method to investigate the effect of clogged arteries and blood flow in the bypass method. In order to simulate as much as possible, the real condition of the artery and the type of blockage were considered in the direction of blood flow. The equations governing blood flow along the hypothetical artery were solved using the finite difference method. According to the effect of dynamic characteristics of blood flow in cardiovascular diseases, velocity profile and pressure against flow were obtained and the effects of various factors such as clogging rate and geometrical parameter were discussed. In order to validate the obtained numerical results, the present results were compared

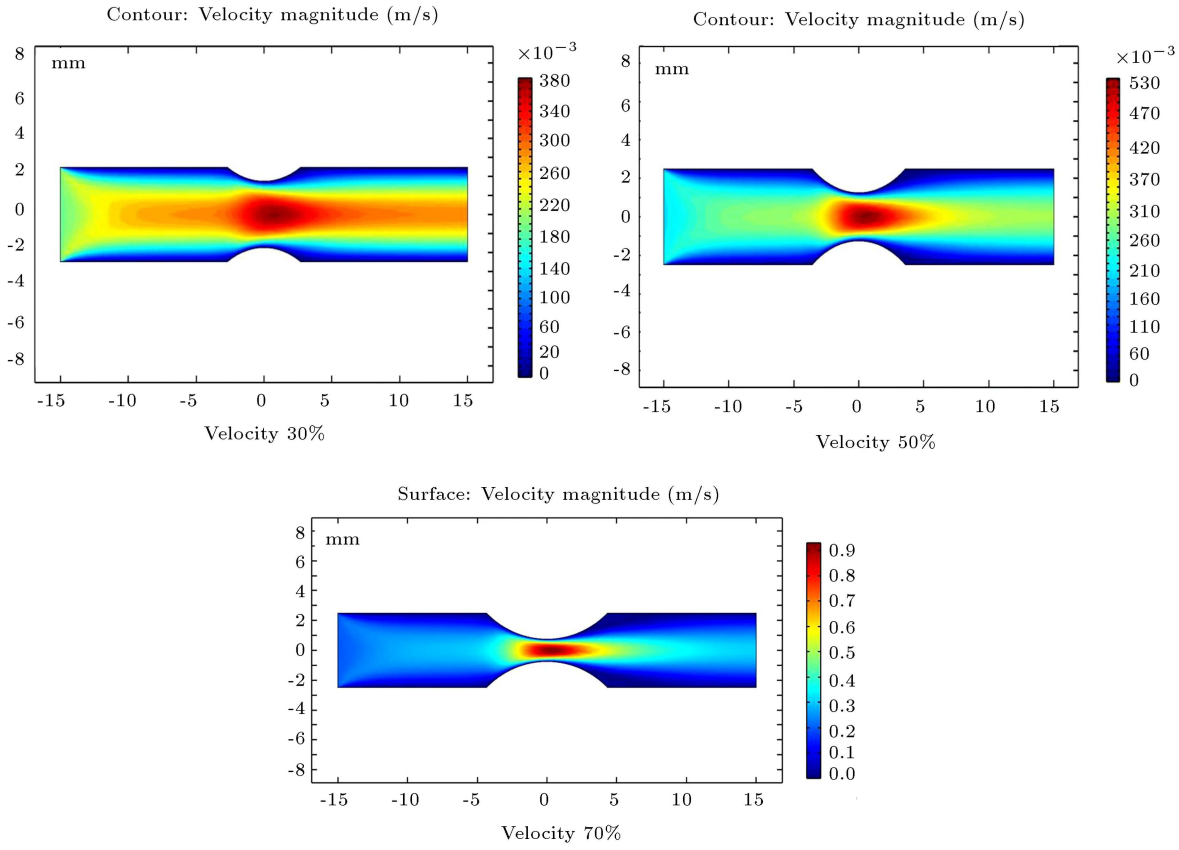

Figure 4. Effect of clogging on blood velocity variation through the vein.

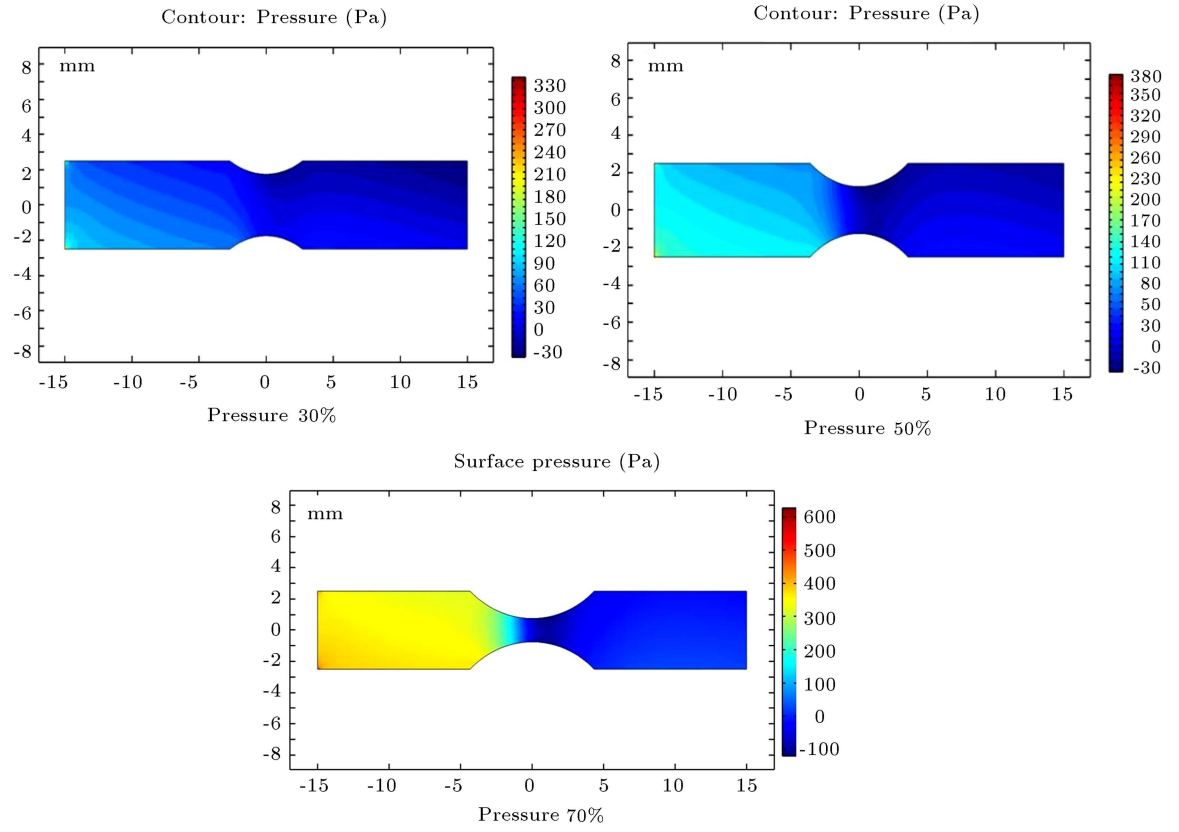

Figure 5. Effect of clogging on blood pressure variation through the vein.

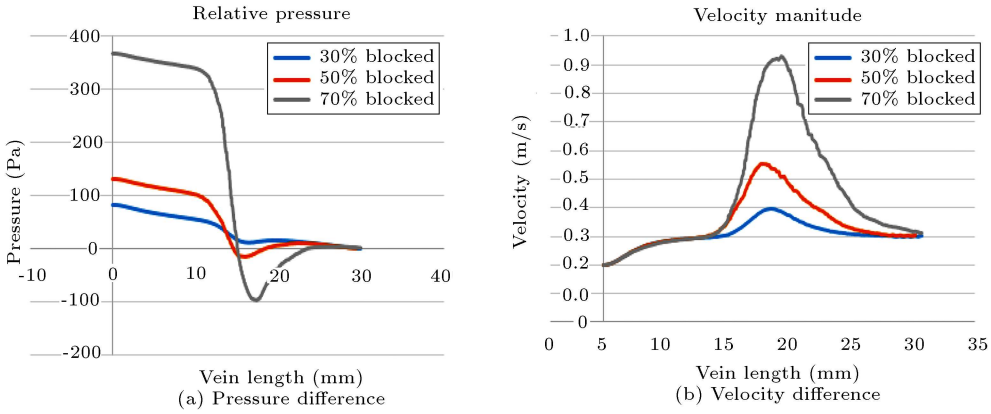

Figure 6. Comparison of the pressure and velocity at different clogging percentiles.

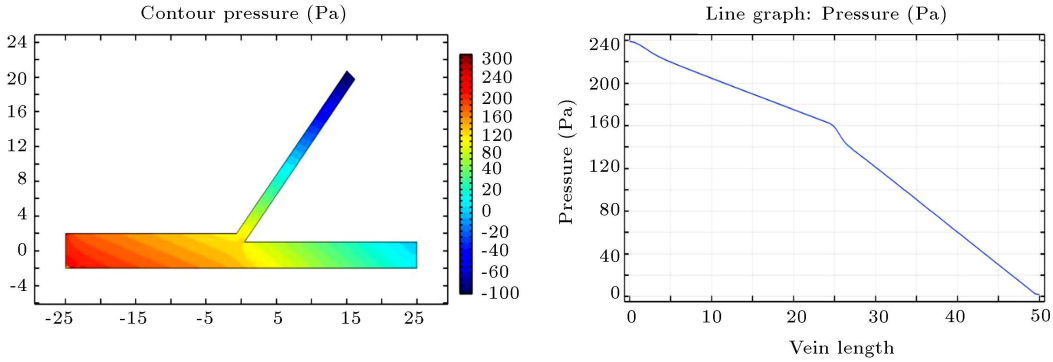

Figure 7. Pressure disturbance by Bypath approach.

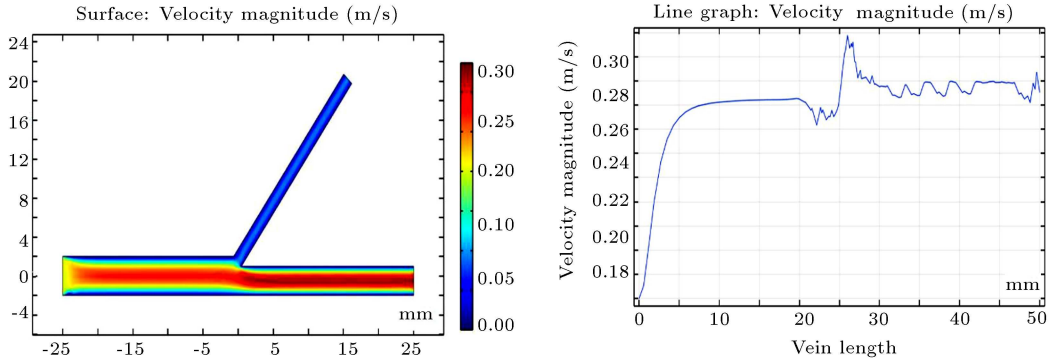

Figure 8. Pressure disturbance by Bypath approach.

with the existing analytical results and good agreement was reached between them. Furthermore, the vessel bypass method was proposed to prevent clogging in arteries, and its results and effect on the rate of clogging in the two-channel state were investigated. As the intensity of clogging increased, the values of rotational velocity and flow resistance increased, while the values of axial velocity, radial velocity, and volumetric flow were reduced.

Acknowledgement

This work was supported by Scientific Research Foundation for Advanced Talents of Guangdong University of Petrochemical Technology (2018rc50).

References

1. Wells, R.G. and Marvin, B. "Measuring SPECT myocardial blood flow at the University of Ottawa Heart Institute", *Journal of Nuclear Cardiology*, **28**(4), pp. 1298–1303 (2021).
2. Suzuki, H., Matsumoto, Y., Sugimura, K., et al. "Impacts of hippocampal blood flow on changes in left ventricular wall thickness in patients with chronic heart failure", *International Journal of Cardiology*, **310**, pp. 103–107 (2020).
3. Zhao, G., Joca, H.C., Nelson, M.T., et al. "ATP-

and voltage-dependent electro-metabolic signaling regulates blood flow in heart", *Proceedings of the National Academy of Sciences*, **117**(13), pp. 7461-7470 (2020).

4. Putra, A.B.W. "Computer technology simulation towards power generation potential from coproduced fluids in south Lokichar oil fields", *International Journal of Communication and Computer Technologies*, **8**(2), pp. 9–12 (2020). DOI:10.31838/ijccts/08.02.03
5. Zharfa, M. and Karimi, N. "Intensification of MILD combustion of methane and hydrogen blend by the application of a magnetic field-a numerical study", *Acta Astronautica*, **184**, pp. 259-268 (2021).
6. Copt, F., Civet, Y., Koechli, C., et al. "Design and manufacturing of an electrostatic MEMS relay for high power applications", *Sensors and Actuators A: Physical*, **321**, p. 112569 (2021).
7. Peskin, C.S. "Numerical analysis of blood flow in the heart", *Journal of Computational Physics*, **25**(3), pp. 220–252 (2021).
8. Sankaran, S., Grady, L.J., and Taylor, C.A. "Systems and methods for virtual contrast agent simulation and computational fluid dynamics (CFD) to compute functional significance of stenoses", Google Patents (2016).
9. Conti, M., Long, C., Marconi, M., et al. "Carotid artery hemodynamics before and after stenting: A patient specific CFD study", *Computers and Fluids*, **141**, pp. 62–74 (2016).
10. Wani, S.D. and Mundada, A. "A review: Emerging trends in bionanocomposites", *International Journal of Pharmacy Research and Technology*, **11**(1), pp. 1–8 (2021).
11. Zhu, G., Wei, Y., Yuan, Q., et al. "Numerical investigation of the hemodynamic environment change in patient-specific intracranial aneurysm with progressive stenosis in unilateral internal carotid artery", *Molecular and Cellular Biomechanics*, **16**(S1), pp. 112–124 (2019).
12. Moshfegh, A., Javadzadegan, A., Zhang, Z., et al. "Effect of aortic spiral blood flow on wall shear stress in stenosed left main coronary arteries with varying take-off angle, stenosis severity and eccentricity", *Journal of Mechanical Science and Technology*, **32**(8), pp. 4003–4011 (2018).
13. Zendehbudi, R. "Effects of non-uniform wall properties on stress distribution in abdominal aortic aneurysm, considering nonlinear constitutive equations", *Scientia Iranica*, **21**(3), pp. 620–627 (2021).
14. Liu, H., Lan, L., Abrigo, J., et al. "Comparison of Newtonian and non-newtonian fluid models in blood flow simulation in patients with intracranial arterial stenosis", *Frontiers in Physiology*, **12**, 718540 (2021). DOI: 10.3389/fphys.2021.718540
15. Heidary, S., Imani, M., and Mostafavi, S.M.A. "Validated and rapid HPLC method for quantification of human serum albumin in interferon beta-1a biopharmaceutical formulation", *Med BioTech Journal*, **1**(01), pp. 26–30 (2022).
16. Rikani, A.S. "Investigation of turbulent fluid flow in the presence of a magnetic field induced dynamic motion of the vessel", *Journal of Research in Science, Engineering and Technology*, **9**(01), pp. 74–94 (2021).
17. Qazani, M.R.C., Asadi, H., Lim, C.P., et al. "Prediction of motion simulator signals using time-series neural networks", *IEEE Transactions on Aerospace and Electronic Systems*, **57**(5), pp. 3383–3392 (2021).
18. El-Hazek, N., Menna, F., and Neveen, A. "Transient flow simulation, analysis and protection of pipeline systems", *Journal of Water and Land Development*, **8**, pp. 98-122 (2020).
19. Ali, A., Hussain, M., Anwar, M.S., et al. "Mathematical modeling and parametric investigation of blood flow through a stenosis artery", *Applied Mathematics and Mechanics*, **42**(11), pp. 1675–1684 (2021).
20. Kadhim, S.K., Al-Azawy, M.G., Ali, S.A.G., et al. "The influence of non-Newtonian model on properties of blood flow through a left coronary artery with presence of different double stenosis", *International Journal of Heat and Technology*, **39**(3), pp. 895–905 (2021).
21. Sahu, N., Sharama, A., Kumar, P.A. "Numerical analysis of blood flow in clogged artery", In *Journal of Physics: Conference Series*, **1964**(6), p. 062102. IOP Publishing (2021).
22. Safi Jahanshahi, A. and Saidi, A.R. "An analytical study on mechanical behavior of human arteries: A nonlinear elastic double layer model", *Scientia Iranica*, **26**(4), pp. 2431–2440 (2019).
23. Dissaneevate, S., Wongsirichot, T., Siriwat, P., et al. "A mobile computer-aided diagnosis of neonatal hyperbilirubinemia using digital image processing and machine learning techniques", *International Journal of Innovative Research and Scientific Studies*, **5**(1), pp. 10–17 (2022). https://doi.org/10.53894/ijirss.v5i1.334
24. Fallahi, H., Shirani, E., and Zohravi, E. "Hemodynamic analysis of coronary artery bypass grafting with elastic walls and different stenoses", *Scientia Iranica*, **28**(2), pp. 773–784 (2021).
25. Ebrahimi, N., Adelian, S., Shakerian, S., et al. "Crosstalk between ferroptosis and the epithelial-mesenchymal transition: Implications for inflammation and cancer therapy", *Cytokine and Growth Factor Reviews*, **64**, pp. 33–45 (2022).
26. Khorsandi, Z., Afshinpour, M., Molaei, F., et al., Design and synthesis of novel phe-phe hydroxyethylene derivatives as potential coronavirus main protease inhibitors", *Journal of Biomolecular Structure and Dynamics*, **30**, pp. 1–9 (2021).
27. Kadhim, S.K., Al-Azawy, M.G., Ali, S.A., et al. "The influence of non-Newtonian model on properties of blood flow through a left coronary artery with presence of different double stenosis", *International Journal of Heat and Technology*, **39**(3), pp. 895-905 (2021).
28. Mojtabavi, L. and Razavi, A. "The effects of addition of copper on the structure and antibacterial properties

of biomedical glasses", *European Chemical Bulletin*, **9**(1), pp. 1-5 (2020).

29. Nadeem, Z.A., Dakhil, S.F., Abdullah, H.M. "Numerical analysis of blood flow through multiple stenosis right coronary artery", *International Journal of Applied Engineering Research*, **13**, pp. 16064–16071 (2018).
30. Delić, M., and Popović, M. "Stability analysis of steel welded tubes forming process using numerical simulations", *Tehnički glasnik*, **15**(2), pp. 298–304 (2021).
31. Ebrahimi, S. and Tahmasebipour, M. "Numerical study of a centrifugal platform for the inertial separation of circulating tumor cells using contraction-expansion array microchannels", *Archives of Razi Institute*, **77**(2), pp. 647–660 (2022).
32. Susanto, A.D., Harahap, R.A., Antariksa, B., et al. "The prevalence and related risk factors of obstructive sleep apnea in heart failure patients at the Indonesian referral hospital for respiratory diseases", *Journal of Natural Science, Biology and Medicine*, **11**(2), pp. 164-174 (2020).
33. Ferguson, S.M., and Langer, L.J. "The US national institutes of health-founding a national biomedical", Innovation Ecosystem, *Journal of commercial biotechnology*, **26**(1), pp. 72–82 (2021).
34. Karjuna, A., Aneela, N., Kotapati, S., et al. "Design of clocked Jk flip flop using air hole structured photonic crystal", *Journal of VLSI Circuits And Systems*, **3**(2), pp. 11-20 (2021). DOI:10.31838/jvcs/03.02.02
35. Mahanthesh, B. and Mackolil, J. "Flow of nanoliquid past a vertical plate with novel quadratic thermal radiation and quadratic Boussinesq approximation: sensitivity analysis", *International Communications in Heat and Mass Transfer*, **120**, pp. 105040 (2021).

Biographies

Wei Long is a Lecturer at Guangdong University of Petrochemical Technology. He holds BS, MS, and PhD degrees in Chemistry from Hunan University of Arts and Sciences, Analytical Chemistry from East China Jiaotong University, Chemical Engineering and Technology from Xiangtan University, respectively. His research interests are adsorption, biomass, catalytic, Nano materials, and characterization technology.

Ria Margiana is a researcher at the Department of Anatomy, Faculty of Medicine, Universitas Indonesia, in Indonesia. She is currently continuing her Master's Programme in Biomedical Sciences at the Faculty of Medicine at Universitas Indonesia, Jakarta, Indonesia. Her research interests include biomedical engineering and bio technology.

Zahraa Haleem Al-qaim is a researcher at the Department of Anesthesia techniques, Al-Mustaqbal University College/Iraq. Her research interests are anesthesia and medical sciences.

Ola Kamal A. Alkadir is a researcher at the Al-Nisour University College/Baghdad/Iraq. His research interests are pathology and medical sciences. He has published more than 10 papers in recent years.

Rosario Mireya Romero Parrais is a Professor at the Department of General Studies, Universidad Continental. Lima, Per. She has published more than 50 scientific publications in journals indexed in SCOPUS, WoS, SciELO, among others and is the author of several book chapters. Her research interests include health science, simulation, and technology application.

Amin Ghanbarzadeh Kojan graduated as a general practitioner at Islamic Azad University of Ardabil in Ardabil, Iran. He worked as Family Medicine in Saravan city of Iran and worked on several projects of Malaria Elimination. Now, he is a general practitioner at Alborz Hospital of Karaj. Research interests are medical sciences and technology application in medical sciences.